

PDM-iRZ-QPSK vs. PS-QPSK at 100 Gbit/s over dispersion-managed links

P. Serena,* N. Rossi, and A. Bononi

Dept. of Information Engineering, Università degli Studi di Parma, 43124 Parma, Italy

[*paolo.serena@unipr.it](mailto:paolo.serena@unipr.it)

Abstract: We compare by simulation the performance of 100Gbit/s PDM-iRZ-QPSK and PS-QPSK transmission both in homogeneous and hybrid QPSK/OOK DM links. We detail the reasons of the overall performance investigating each nonlinear effect (SPM, XPM and XPolM) individually. Moreover, we compare the accuracy of the noise loading method with the more realistic use of noisy in-line amplifiers. Results shows that i) PDM-iRZ-QPSK and PS-QPSK have same reach in both homogeneous and hybrid setups, ii) correct simulations must include distributed ASE.

© 2012 Optical Society of America

OCIS codes: (060.2330) Fiber optics communications; (060.1660) Coherent communications.

References and links

1. M. Karlsson and E. Agrell, "Which is the most power-efficient modulation format in optical links?" *Opt. Express* **17**(13), 10814–10819 (2009).
2. E. Agrell and M. Karlsson, "Power-efficient modulation formats in coherent transmission systems," *J. Lightwave Technol.* **27**(22), 5115–5126 (2009).
3. P. Poggiolini, G. Bosco, A. Carena, V. Curri, and F. Forghieri, "Performance evaluation of coherent WDM PS-QPSK (HEXA) accounting for non-linear fiber propagation effects," *Opt. Express* **18**(11), 11360–11371 (2010).
4. P. Serena, A. Vannucci, and A. Bononi, "The performance of polarization switched-QPSK (PS-QPSK) in dispersion managed WDM transmissions," in *Proc. ECOC 2010, Torino, Italy*, (2010). Paper Th.10.E.2.
5. D. S. Millar, D. Lavery, S. Makovejs, C. Behrens, B. C. Thomsen, P. Bayvel, and S. J. Savory, "Generation and long-haul transmission of polarization-switched QPSK at 42.9 Gb/s," *Opt. Express* **19**(10), 9296–9302 (2011).
6. C. Xie, "Interchannel nonlinearities in coherent polarization-division-multiplexed quadrature-phase-shift-keying systems," *IEEE Photon. Technol. Lett.* **21**(5), 274–276 (2009).
7. O. Bertran-Pardo, J. Renaudier, G. Charlet, P. Tran, H. Mardoyan, M. Salsi, M. Bertolini, and S. Bigo, "Insertion of 100Gb/s coherent PDM-QPSK channels over legacy optical networks relying on low chromatic dispersion fibres," in *Proc. IEEE Globecom*, (2009).
8. A. Bononi, N. Rossi, and P. Serena, "Transmission limitations due to fiber nonlinearity," in *Proc. OFC-NFOEC 2011, Los Angeles, CA*, (2011). Paper OWO7.
9. P. Serena, M. Bertolini, and A. Vannucci, "Optilux toolbox," (2009). [online] www.optilux.sourceforge.net.
10. P. Serena, N. Rossi, O. Bertran-Pardo, J. Renaudier, A. Vannucci and A. Bononi, "Intra- versus Inter-channel PMD in Linearly Compensated Coherent PDM-PSK Nonlinear Transmissions," *J. Lightwave Technol.* **29**(11), 1691–1700 (2011).
11. P. Johannisson, M. Sjödin, M. Karlsson, H. Wymeersch, E. Agrell, and P. A. Andrekson, "Modified constant modulus algorithm for polarization-switched QPSK," *Opt. Express* **19**(8), 7734–7741 (2011).
12. A. J. Viterbi and A. M. Viterbi, "Nonlinear estimation of PSK-modulated carrier phase with application to burst digital transmission," *IEEE Trans. Inf. Theory* **29**(4), 543–551 (1983).

1. Introduction

Polarization division multiplexing (PDM) has become the standard for 100 Gbit/s optical links. Besides PDM quadrature phase shift keying (PDM-QPSK), polarization switched QPSK (PS-QPSK) was recently introduced as a promising alternative because of its improved sensitivity

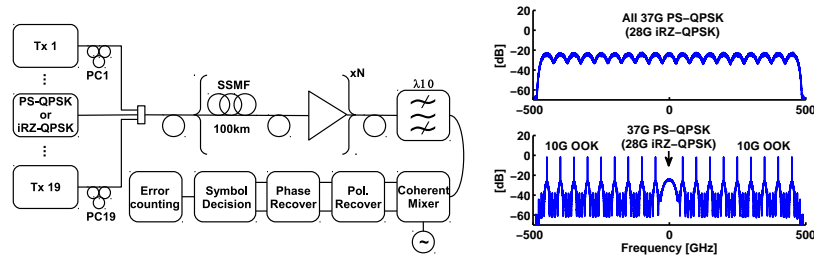


Fig. 1. Left: Simulated $N \times 100$ km, 112 Gbit/s DM30 link. Right: 19 channels spectra in the homogeneous (top) and hybrid (bottom) cases.

against additive Gaussian noise [1, 2]. Such a benefit comes at the expense of an increased symbol rate. For instance, at 112 Gbit/s one needs a symbol rate of 28 Gbaud for PDM-QPSK and 37 Gbaud for PS-QPSK. The resilience of PS-QPSK against amplified spontaneous emission (ASE) noise has been shown to be paired with a larger tolerance against Kerr effects with respect to PDM-QPSK [3–5] and the reason is related to both the increased symbol distance and the increased symbol rate that helps averaging out nonlinear distortions generated along the line. The tolerance of PDM-QPSK to nonlinear effects can be improved by using interleaved return to zero (iRZ) pulse shaping [6]. iRZ is created by introducing a delay of half a symbol time between the polarization tributaries, thus obtaining a binary-alternating state of polarization (SOP) that improves the tolerance against nonlinear cross-polarization modulation (XPolM) [6, 7].

In this work we present a simulation-based comparison of PDM-iRZ-QPSK versus PS-QPSK at 112 Gbit/s over dispersion managed (DM) links, both with format *homogeneous* channels, and with a *hybrid* scheme with a central QPSK channel surrounded by 10Gb/s on-off keying (OOK) channels. We will use the nonlinearity-decoupling method [8] to understand the role of the main nonlinearities, namely, self-phase modulation (SPM), cross-phase modulation (XPM) and XPolM. We also investigate the accuracy of the fast noise-loading simulation technique against the computationally-heavy true case of distributed noise generation at in-line amplifiers.

We initially tried to speed up simulations for these systems by using a memoryless polarization demultiplexer in place of the standard CMA equalizer, as we already did for PDM-NRZ-QPSK in previous time-consuming simulations of the nonlinear threshold [8]. We later realized that for iRZ such a trick does not work, and we explain why in the Appendix.

2. Simulations setup

The simulated DM optical link was composed of N standard single mode fiber (SSMF) spans of 100 km each, with a typical in-line residual dispersion $D_{in} = 30$ ps/nm/span. Before transmission we inserted a pre-compensating fiber of $-369 - (N - 1)D_{in}/2$ ps/nm [8]. The value of N was varied in the range 20 to 60. At the end of the link, an ideal post-compensating fiber set the total cumulated dispersion to zero. Fiber propagation was implemented with the separate-field solution [9] of the Manakov equation in the worst-case of no polarization mode dispersion (PMD) [10]. ASE noise was either inserted along the line with amplifiers having a noise figure of 6 dB or into a unique white noise source before detection (noise loading). The first approach accounts for nonlinear phase noise (NLPN) generated along the line.

The transmitter consisted of 19 wavelength division multiplexed (WDM) synchronous channels, with 50 GHz spacing, each modulated with 1024 random symbols, at 32 samples per symbol, whose format was either 112 Gbit/s PS-QPSK, or 112 Gbit/s PDM-iRZ-QPSK or 10 Gbit/s OOK, according to the homogeneous or hybrid WDM scheme, as depicted by the spectra

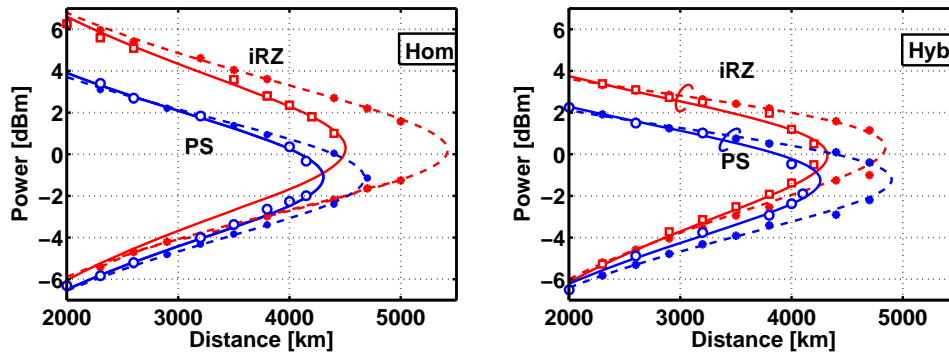


Fig. 2. Power that yields Q-factor=8.5 dB vs. transmission distance for the given DM link with 30 ps/nm. *Solid* lines: distributed noise (NLPN). *Dashed* lines: End-link noise loading. Left: Homogeneous setup. Right: Hybrid setup.

in Fig. 1. In the hybrid scheme the surrounding OOK channels had 4 dB less power than the central test channel. The SOP of each carrier was randomly selected over the Poincaré sphere at each run. The optical pulses in PS-QPSK were non-return to zero while for PDM-iRZ-QPSK the pulse shaping was obtained by an RZ carver. Before multiplexing, each channel was filtered by a 2nd order super-Gaussian filter of bandwidth 0.4 nm. Before detection we used an optical filter of bandwidth 1.8R that extracted the central WDM channel, R being the symbol rate.

The digital signal processing unit of the coherent receiver accounted for: low pass filtering over a bandwidth of 0.7R GHz, sampling at 2 samples per symbols, polarization recovery through a 7-taps CMA [11], phase-recovery with the Viterbi and Viterbi (V&V) algorithm [12], decision and finally differential decoding [4]. At each power we tested both a V&V with 27 and 7 taps and used the best value. In the PS-QPSK case we sequentially detected the polarization-switch bit and then the remaining QPSK bits. In each setup we measured the Q-factor by Monte Carlo simulations, counting at least 400 errors except for points at very large Q-factor and thus out of interest. With NLPN we changed the random seed at each run, while in the noise loading case we always averaged over 10 seeds. All simulations were performed with Optilux [9].

3. Results

We started by calculating the transmitted channel power that yields a Q-factor of 8.5 dB at different transmission distances. At each distance we have two values, one in the linear ASE dominated regime, the other in the nonlinear regime. Such powers are reported in the 8.5 dB Q-factor contours of Fig. 2. Solid lines refer to simulations with noisy in-line amplifiers, while dashed lines refer to simulations with the noise loading method. We note that noise loading is inaccurate, particularly for homogeneous-iRZ where the largest reach is over-estimated by 1000 km. With realistic distributed noise, indeed, both formats reach roughly the same 4000 km maximum distance, iRZ showing a slightly poorer linear performance compared to PS [2] but a much larger nonlinear tolerance, and thus overall a larger power tolerance.

We explored the reasons behind the penalty by calculating the Q-factor versus power through the nonlinearity decoupling method [8]. Figure 3 shows such bell curves, calculated only with distributed noise at 4000 km, i.e., around the best reach in each case. The impact of each nonlinear effect acting alone is indicated by the corresponding name. The curve labeled “WDM” refers to the real case with all nonlinearities. Note that at each power the V&V length was set equal to the best one of the WDM setup, which may be non-optimal for the specific nonlinear

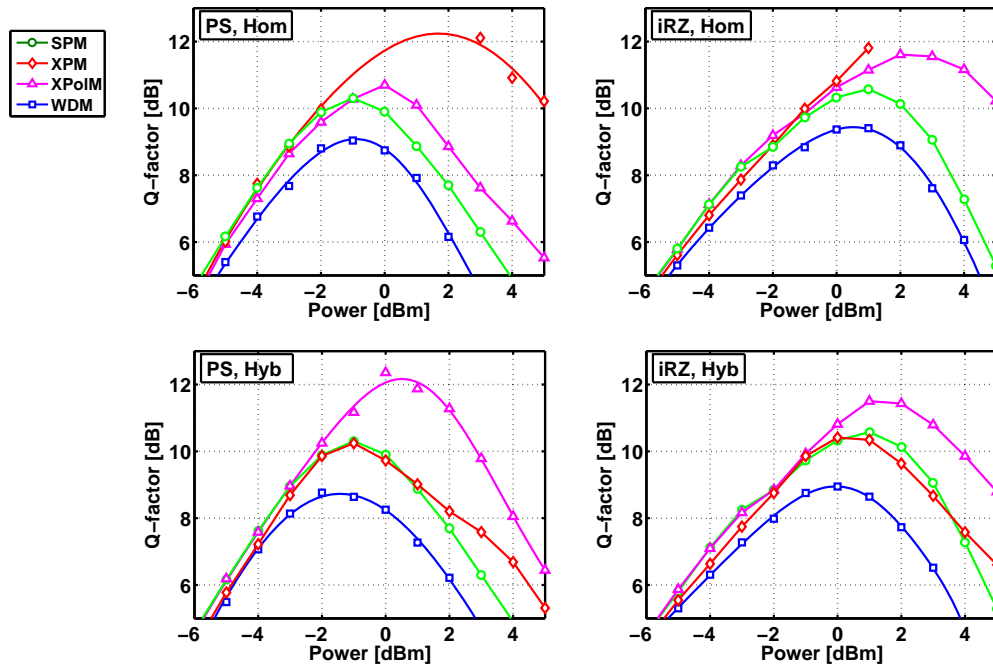


Fig. 3. Q-factor (with nonlinearity decoupling) vs power for (top row) homogeneous scheme, (bottom row) hybrid scheme, after 4000km of the DM map. WDM: SPM+XPM+XPolM. Solid lines: data interpolation.

effect operating alone.

In the homogeneous case (top-row) the SPM is the largest nonlinear effect for both formats. In DM maps such SPM is stronger because of the NLPN due to the interaction of signal and ASE [8], as visible in Fig. 2. As expected, PDM-iRZ-QPSK has a larger tolerance to XPolM since its binary SOP alternates periodically between two orthogonal states, while PS-QPSK performs the same alternation in a random way. Moreover, PDM-iRZ-QPSK is more robust against all nonlinearities in the descending part of the bell curve. XPM is larger in PS-QPSK because of the larger amplitude fluctuations induced by the transmission filter that translate in a greater XPM. However, XPM is negligible in both formats.

In the hybrid case XPM becomes higher in both cases because of the amplitude fluctuations of the OOK. In such a case a short V&V window can better smooth phase fluctuations induced by the highly correlated XPM: for instance, we measured an improvement of the best WDM Q-factor of $\Delta = 1.2$ dB for both formats when decreasing from 27 to 7 V&V taps, while we measured $\Delta = 0.3$ dB in the homogeneous case. For PS-QPSK, XPolM is reduced compared to the homogeneous case mainly because of the reduced power of the OOK channels.

4. Conclusions

We compared 112 Gbit/s PDM-iRZ-QPSK vs. PS-QPSK on DM SSMF links. Our main results show that in both an homogeneous and hybrid scenario the two formats have roughly the same reach. Moreover, we verified that simulations based on noise loading are inaccurate, especially for PDM-iRZ-QPSK in homogeneous setups. Finally we showed in the Appendix that iRZ shaping does require the equalizing capability of a multi-tap CMA even in absence of PMD,

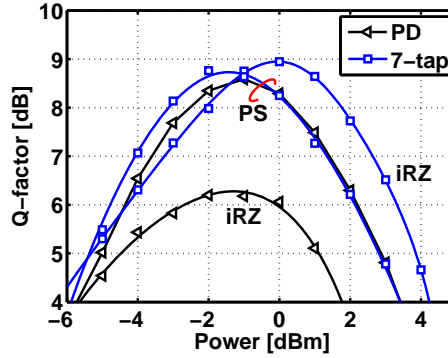


Fig. 4. Q-factor after 4000 km for Hybrid setup with polarization demultiplexer (PD)- (triangles) or 7-tap CMA (squares) . While for the NRZ pulses of PS-QPSK CMA and PD give similar performance, for PDM-iRZ-QPSK the PD is strongly penalizing.

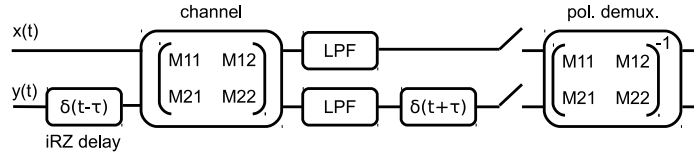


Fig. 5. Simplified system model. LPF is the ADC filter.

while normally simulations can be made faster using a single-tap polarization demultiplexing.

Appendix

In the previous simulations we used a 2 sample per symbol fractionally spaced CMA-driven equalizer with 7 taps. Since PMD and the residual dispersion of the link were zero, the CMA essentially recovered linear filtering distortions as well as the average polarization rotation induced by XPolM. In an early set of simulations we just recovered the polarization axes by a memoryless data-aided polarization demultiplexer (PD), equivalent to a 1-tap CMA, in an attempt to speed up the time-consuming simulations [8] . As shown in Fig. 4, for PS-QPSK we did not observe any significant change between the 7-tap CMA and the PD case. Surprisingly, with PDM-iRZ-QPSK we noted a significant performance degradation using the PD, and this appendix explains why.

Assume the simplified scheme of Fig. 5 where the channel is represented by a memoryless unitary matrix, and the polarization demultiplexer just inverts such a matrix. The lowpass filter (LPF) with impulse response $h(t)$ models the analog digital converters (ADC) response. $x(t)$ and $y(t)$ are the two PDM-QPSK tributaries, while the Dirac delta $\delta(t \pm \tau)$ indicates the impulse response of a delay line of τ seconds. This scheme works both with/without pulse interleaving: in the first case $\tau = 0$, while for iRZ τ is half a symbol time: $\tau_{iRZ} = T/2$. After sampling at $t = t_k$, for iRZ shaping we have the following signals:

$$\begin{bmatrix} x_2(t_k) \\ y_2(t_k) \end{bmatrix} = \begin{bmatrix} M_{11} & 0 \\ 0 & M_{22} \end{bmatrix} \begin{bmatrix} x(t) \otimes h(t)|_{t_k} \\ y(t) \otimes h(t)|_{t_k} \end{bmatrix} + \begin{bmatrix} 0 & M_{12} \\ M_{21} & 0 \end{bmatrix} \underbrace{\begin{bmatrix} x(t + \frac{T}{2}) \otimes h(t)|_{t_k} \\ y(t - \frac{T}{2}) \otimes h(t)|_{t_k} \end{bmatrix}}_{\text{crosstalk}} \quad (1)$$

where \otimes denotes convolution. Due to the presence of the crosstalk term, Eq. (1) in general is

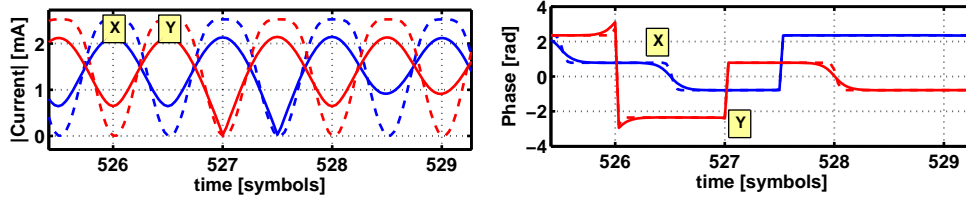


Fig. 6. iRZ electric current at the output of the LPFs for polarization X and Y. Dashed: LPF of infinite bandwidth. Solid: LPF of bandwidth $0.7R$.

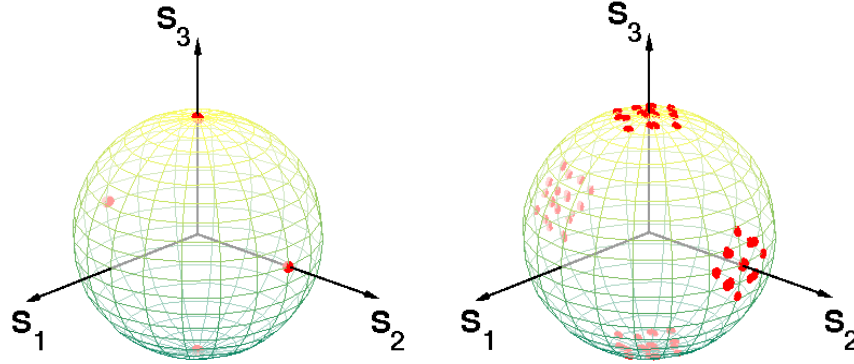


Fig. 7. SOP over the Poincaré sphere without (left) and with (right) pulse interleaving of a PDM-QPSK signal after reception with PD. The SOP spreading with interleaving can be removed using either a larger bandwidth ADC or a CMA equalizer.

not a unitary transformation applied to $[x(t), y(t)]$. We expect the crosstalk to spread the SOP over the Poincaré sphere, thus compromising the demultiplexing.

Without interleaving it is $\tau = 0$, hence we have the following:

$$\begin{bmatrix} x_2(t_k) \\ y_2(t_k) \end{bmatrix} = \begin{bmatrix} M_{11} & M_{12} \\ M_{21} & M_{22} \end{bmatrix} \begin{bmatrix} x(t) \otimes h(t)|_{t_k} \\ y(t) \otimes h(t)|_{t_k} \end{bmatrix}.$$

For practical not too narrow LPF, the net result of filtering is essentially an energy loss around sampling times, such that $x(t) \otimes h(t)|_{t_k} \simeq x(t_k)c$ and $y(t) \otimes h(t)|_{t_k} \simeq y(t_k)c$, being c a constant. See Fig. 6 for example. But a constant like c impacts equally signal and noise, thus leaving a “clean” SOP over the Poincaré sphere as for a generic rotation. Figure 7 (left) confirms the claim showing that there is no SOP spreading, i.e., no polarization crosstalk.

Figure 7 (right) shows that with iRZ instead the SOP spreads into a grid. This is so, since the interfering symbols can be combined into a finite number of ways. A SOP spreading would appear even with NRZ-PDM-QPSK when using very narrow LPF.

In such cases a simple polarization demultiplexer is not sufficient to correctly recover the PDM signal, hence a CMA equalizer with sufficiently many taps is needed.